The Globally Trapped Future: A Fate for Black Holes and Wormholes

Yi-Bo Liang and Hong-Rong Li* School of Physics, Xi'an Jiaotong University, Xi'an 710049, China (Dated: November 26, 2025)

A new general dynamical metric is obtained through a generalization of the Schwarzschild foundations, explicitly providing the global causal structure and trapping horizons and establishing three possible fates of the spacetime: those without a globally trapped future; those without global trapping but containing bounded, Cauchy-foliated trapped regions; and those with a future that becomes completely globally trapped. This framework is illustrated through the evolution of a geometrically Schwarzschild-like black hole and a horizonless wormhole, thereby establishing the final, globally trapped fate as a novel theoretical possibility.

Introduction. Black holes are not only a cornerstone prediction of Einstein's gravity but also an established astrophysical reality. The Schwarzschild black hole [1, 2] and its distinct bifurcate horizon provide the essential framework for black holes in general relativity; nevertheless, it possesses a spacetime singularity [3–5] that indicates the theory's breakdown, thereby preventing classical predictions, information retrieval, or a smooth extension of the spacetime. Contemporary research extends this paradigm to regular black holes [6–25]—non-singular horizoned objects—motivating a fundamental question: how do such objects evolve dynamically?

Influential models and analyses [26–33] suggest that a black hole may theoretically transition into a traversable wormhole, and vice versa. This framework enables a reexamination of the relationship between wormholes and black holes through an analysis of the transmissibility of their trapping horizons. Indeed, the Schwarzschild black hole can be reinterpreted as a wormhole with unidirectional traversability, where the central singularity blocks all passage. Scientific inquiry extends beyond the mere interconversion of these objects to encompass their ultimate fate. A pivotal question is whether, within a finite time, they will eventually engulf the entire future spacetime.

By generalizing the foundations of the Schwarzschild metric, we derive a new dynamical metric that reveals three possible fates of spacetime. This metric directly yields the global causal structure and trapping horizons, leading to three distinct causal fates of the spacetimes: those without a globally trapped future; those without global trapping but containing bounded, Cauchy (surface)-foliated trapped regions; and those with a future (of a globally hyperbolic spacetime after a finite time) that becomes completely globally trapped that becomes completely globally trapped. Corresponding examples, illustrating the evolution of a geometrically Schwarzschild-like black hole (GSLBH) and an initially horizonless wormhole, are presented in the following. Notably, the third fate—a fully future-trapped spacetime—presents a novel theoretical possibility for the evolution of a GSLBH, which necessitates careful consideration.

Theoretical Framework. In this study, we will inherit the characteristics of maximally extended Schwarzschild black hole (MESBH) and broaden the allowable range of the energy momentum tensor to obtain a general nonstationary spacetime. A general non-stationary spherically symmetric metric is

$$ds^{2} = -C(T, X)dT^{2} + D(T, X)dX^{2} + R^{2}(T, X)d\Omega^{2}.$$
 (1)

As usual, a coordinate condition is imposed to eliminate the diagonal term g_{TX} , leaving one coordinate condition remaining. Typically, this residual coordinate condition is used to make R(T,X) a radial coordinate. Here, however, inspired by the Kruskal coordinates of MESBH, we assume globally that A(T,X) = C(T,X) = D(T,X), so that the two-dimensional Lorentzian orbit space M/SO(3) is conformally flat. This choice also fixes the residual coordinate freedom. Since $\{T,X,\theta,\varphi\}$ are taken as global coordinates, and the spacetime is required to be regular and globally hyperbolic, the function A must possess no zeros. The spacetime is taken to have the topology $\mathbb{R}^2 \times S^2$ with R>0 and $T,X\in\mathbb{R}$, ensuring regularity and preserving the topological features of MESBH.

Define $t\equiv T, r\equiv X,$ and require that the energy–momentum tensor be diagonal in these coordinates. Then, we have

$$\partial_t A \partial_r R + \partial_r A \partial_t R - 2A \partial_{t,r} R = 0. \tag{2}$$

A sufficient condition for the solvability of the equation for a general R, namely the separability of the derivative ratio $\partial_t R/\partial_r R = P(t)/Q(r)$, leads to the general solution $R = \mathcal{R}(f(r) + h(t))$. This framework incorporates the separable ansatz R = j(r)k(t) via the identification $\mathcal{R}(f+h) \equiv \exp(f+h), f(r) = \ln j(r)$, and $h(t) = \ln k(t)$. Therefore, Eq. (2) can be solved to yield

$$A = F(f - h)\mathcal{R}'(f + h), \ R = \mathcal{R}(f + h), \ A > 0,$$
 (3)

where $\mathcal{R}' \equiv d\mathcal{R}/d(f+h)$. To preserve the time-reversal symmetry and the discrete isometry $X \to -X$ of the MESBH, we require $f = f(r^2)$ and $h = h(t^2)$, with the additional requirement that both functions are smooth.

A GSLBH is then defined by the condition that its trapping horizons are bifurcated and null at the point t=r=0.

The two radial null geodesic tangent vectors are defined as $k_{\pm}^{a} \equiv (1/\sqrt{2A})((\partial/\partial t)^{a} \pm (\partial/\partial r)^{a})$. Their expansions, $\theta_{k_{\pm}} = h^{ab}\nabla_{a}k_{\pm a}$, are computed using the induced metric $h_{ab} \equiv g_{ab} + k_{+a}k_{-b} + k_{-a}k_{+b}$, yielding the explicit expressions: $\theta_{k_{\pm}} = \sqrt{2/A(\mathcal{R}'/\mathcal{R})}(\partial_{t}h \pm \partial_{r}f)$.

Given that A>0 and F,\mathcal{R}' are functions of independent variables, they must be nonzero and thus possess definite signs. General results for the spacetime in Eq. (3) can be established assuming $\mathcal{R}'>0$, because the case $\mathcal{R}'<0$ can be transformed into the former by defining $\mathcal{R}(f+h)=\mathcal{R}(-(-f-h))\equiv\tilde{\mathcal{R}}(\tilde{f}+\tilde{h})$ with $\tilde{f}\equiv -f, \tilde{h}\equiv -h$, ensuring $\tilde{\mathcal{R}}'>0$. Consequently, we have $\text{sign}[\theta_{k_{\pm}}]=\text{sign}[\partial_t h\pm\partial_r f]$. The trapped regions are precisely those where $\partial_t h\pm\partial_r f<0$. This work investigates the existence of future trapped regions—a condition implying $\text{sign}[\theta_{k_+}+\theta_{k_-}]=\text{sign}[\partial_t h]<0$ as $t\to +\infty$. The subsequent analysis is dedicated to this problem, employing the simplifying assumption that $\partial_t h<0$ for t>0.

- (i) The spacetime will not be entirely trapped in the future if $\sup |\partial_r f| = +\infty$ or if $\sup |\partial_r f| = \delta$ provided that $\lim_{t\to +\infty} \partial_t h \geq -\delta$.
- (ii) Any spacetime region defined by $t_0 < t < t_1$ and satisfying $\sup |\partial_r f| \leq \delta$ and $\partial_t h \leq -\delta$ is trapped. It follows that one or more such trapped regions can exist.
- (iii) The remaining scenario is characterized by the asymptotic conditions $\partial_t h \leq -\delta$ as $t \to +\infty$ and $\sup |\partial_r f| \leq \delta$. Integration of the condition on h implies $h(t^2) < h(t_0^2) \delta(t t_0)$, that is, $\lim_{t \to +\infty} h = -\infty$. Consequently, the argument $x = f + h \to -\infty$, decreasing monotonically. Given $\mathcal{R} > 0$ and $\mathcal{R}' > 0$, $\mathcal{R}(x)$ must approach its infimum $L \geq 0$ as $x \to -\infty$. Similarly, it can be verified that $\mathcal{R}' \to 0^+$ as $x \to -\infty$. Therefore, if the spacetime is entirely future-trapped, the areal radius \mathcal{R} approaches its minimum value L as $t \to \infty$. Special care is required when $\mathcal{R}' \to 0^+$, as this may lead to $A \to 0^+$, which could prevent the coordinates $\{t, r, \theta, \varphi\}$ from covering the entire spacetime.

The spacetime precludes the definition of conformal spacelike boundaries at temporal infinity $(t \to \infty)$, and thus, due to the condition $g_{tt} = -g_{rr}$, also precludes conformal timelike boundaries at spatial infinity $(r \to \infty)$. Introducing the light-cone coordinate $u \equiv t - r$, we observe that $x \to x_0$ or $x \to -\infty$ (since $\partial_t x < 0$) as $t \to +\infty$ along lines of constant $u = u_0$, therefore, $\mathcal{R} \to \mathcal{R}(x_0) \geq L$. Consequently, conformal null boundaries cannot be defined for this spacetime. Therefore, this spacetime cannot be asymptotically flat, but nothing prevents it from being globally hyperbolic. We emphasize that the coordinates $\{t, r, \theta, \varphi\}$ are required to be global; hence, possible spacetime extensions are not considered in this analysis.

We thus identify three possible fates for the spacetime.

The time reversal symmetry of h, combined with the condition $\partial_t h < 0$ for t > 0, implies a bounce in the constantr slices. This bounce behavior and the known relations between black holes and wormholes prompt the construction of corresponding models from specific solutions, including static wormholes and exact non-stationary solutions which incorporate a bounce. We emphasize that these exact solutions arise from a theoretical framework comprising a partly phantom field and a nonlinear electrodynamics (NED) field, as given by the action

$$S = \int_{M} \epsilon \left[R - p(\phi) \nabla^{a} \phi \nabla_{a} \phi - V(\phi) - \mathcal{L}(F) \right], \quad (4)$$

with $c=G=\hbar=4\pi\varepsilon_0=1$. The combination of these two fields is inspired by [23]. Here, $p(\phi)$ represents the parametrization freedom of the scalar field, where a sign change in p corresponds to a switch between canonical and phantom regimes. Moreover, the NED field is magnetic, with $F_{ab}=g\sin\theta\mathrm{d}\theta\wedge\mathrm{d}\varphi$ and $F=F_{ab}F^{ab}=2g^2/\mathcal{R}^4$, where g is the magnetic charge.

For both static metrics $(A = A(r^2), \mathcal{R} = \mathcal{R}(r^2))$ and non-stationary metrics $(A = A(t^2), \mathcal{R} = \mathcal{R}(t^2))$, the field sources are given by

$$\phi = \phi_s, \ p = G_{tt} + G_{rr}, \ V = \frac{2G_{tt}}{A} + \frac{sp}{A} - L,$$
 (5)

$$\mathscr{L}_F F = \frac{1+s}{2} \frac{G_{tt}}{A} - \frac{1-s}{2} \frac{G_{rr}}{A} - \frac{G_{\theta\theta}}{\mathcal{R}^2}, \ \mathscr{L}_F \equiv \frac{\mathrm{d}\mathscr{L}}{\mathrm{d}F}, \ (6)$$

where the parameter s takes the value +1 (with $\phi_{+1} = r$) and -1 (with $\phi_{-1} = t$), respectively. In both cases, R must be monotonic and continuous for r^2 or t^2 . This condition is essential for obtaining the inverse relations $r^2(F)$ or $t^2(F)$, and thus for solving for \mathcal{L} .

An asymptotically flat spacetime. For a MESBH near its horizon $(T \approx \pm X)$, the following approximation holds: $\mathcal{R} \approx 2M(1+X^2/\mathrm{e}-T^2/\mathrm{e})$. The simplest \mathcal{R} in our model that exhibits this behavior—and which reduces to the well-known Ellis–Bronnikov wormhole for h=0—is $f=\sqrt{r^2+a^2},\ h=m/(1+kt^2),\ \mathcal{R}=f+h$. Therefore, $\mathcal{R}'=1$, and hence we can set F=1. The metric is

$$ds^{2} = -dt^{2} + dr^{2} + \left(\frac{m}{1 + kt^{2}} + \sqrt{r^{2} + a^{2}}\right)^{2} d\Omega^{2}, \quad (7)$$

where $m, k \geq 0, a > 0$. The spacetime is regular and reduces to a wormhole (s = +1) in the three independent limits: $m = 0, t \to 0$, or $t \to \infty$. It reduces to a bounce (s = -1) in the limit: $r \to 0$, in all cases keeping terms up to O(1). Since the spacetime is asymptotically flat at null infinities [34] and the vector field $(\partial/\partial t)^a$ is asymptotically Killing, it follows that the Bondi energy vanishes.

The throat measures a + m at t = r = 0, with a representing its global minimum. The causal nature of the marginally trapping horizon is determined by its dual normal covector $n_a \equiv (d\theta_{k_+})_a$, with analysis confined

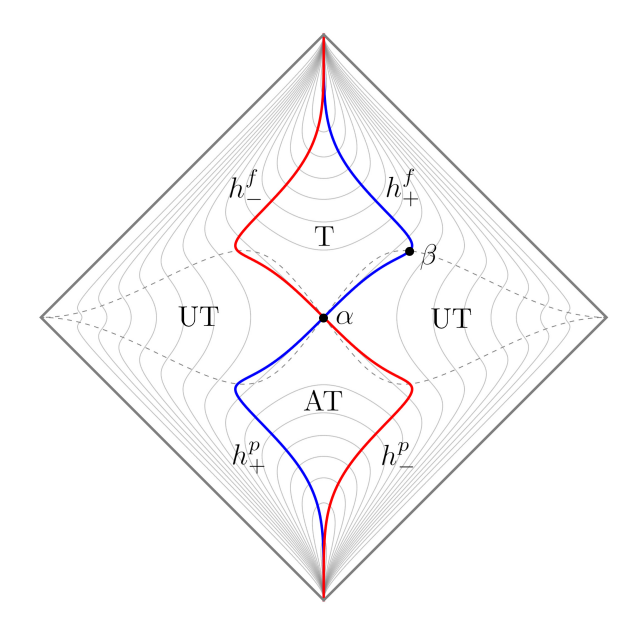


FIG. 1: The Penrose diagram for parameters a=0.4, m=1.4, k=1/(2am). Regions: A (trapped), AT (anti-trapped), UT (untrapped). Blue and red lines indicate marginally trapping horizons of k_+^a and k_-^a , thick and thin gray lines denote null infinities and constant \mathcal{R} surfaces (larger \mathcal{R} closer to null infinity). The null energy condition (NEC) and the strong energy condition (SEC) are satisfied in the region between the two dashed lines.

to k_+^a by symmetry. For t > 0, the horizon is null at no more than three points, while it becomes timelike as $t \to +\infty$. From $\partial_t h(r^2) + \partial_r f(r^2) = 0$ as $t \to 0^+$, the approximation $r/a + O(r^3) = 2mkt + O(t^3)$ implies that the horizon's character (null, spacelike, or timelike) in this limit is dictated by the value of mk.

The special case 2mk = 1/a yields a GSLBH as $t \rightarrow 0^+$; given sup $\partial_r f = 1$, a Cauchy-foliated region is trapped if $\inf \partial_t h < -1$, which is equivalent to $m^2k \geq (4/3)^3$. The Penrose-Carter diagram illustrating the evolution of the GSLBH is shown in Figs. 1 and 2. In Fig. 1, the horizons h_{+}^{f} and h_{-}^{f} initially expand and subsequently contract. The surface h_{+}^{f} is a future outer trapping horizon (FOTH) that is null at α, β , α, β in (α, β) , and timelike elsewhere; thus, its one-way traversable spacelike segment (with positive flux into it) defines a black hole horizon. The remaining timelike portion of h_{+}^{f} (with negative flux into it) is bidirectional traversable, corresponding to a wormhole horizon. The transformation $t \to -t, r \to -r$ clarifies the properties of h_{+}^{p} and h_{-}^{f} . In summary, the spacetime—initially containing a GSLBH—first undergoes accretion, then experiences a classical analogue of evaporation, and finally makes a definitive transition into a traversable wormhole. The collections of the throats and bounces are the

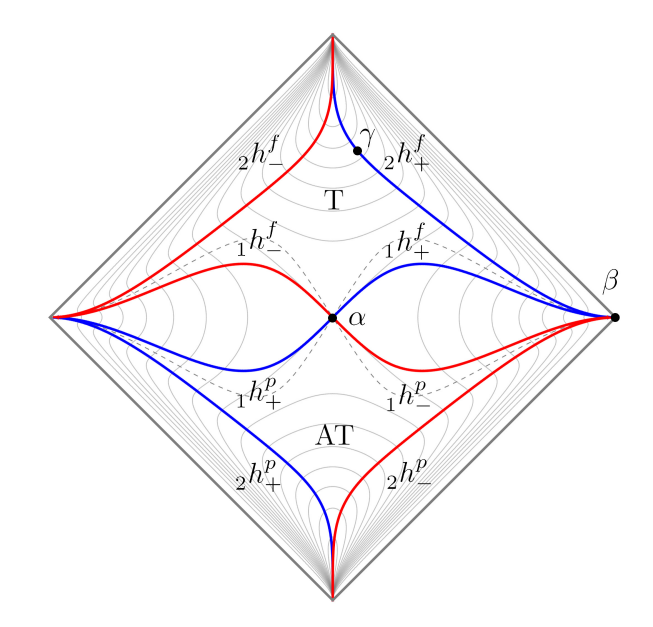


FIG. 2: Penrose diagram for a=0.4, m=2, k=1/(2am). $\rho \geq 0$ inside the regions enclosed by the four dotted lines. The label UT is not shown.

regions $T \cup AT$ and UT, respectively.

As shown in Fig. 2, a black hole first traps a Cauchy-foliated region and subsequently evaporates into a wormhole. This trapped region is bounded by the horizons $_1h_+^f, _2h_+^f, _1h_-^f$ and $_2h_-^f$. The spacelike segment (β, γ) of $2h_-^f+$ —which is null at γ —is a future inner trapping horizon (FITP) (with negative flux into it).

To obtain an evolution of an initially horizonless wormhole, just replace of kt^2 in h with lt^4 . Here, "horizonless" indicates that, at t=r=0 and for fixed θ, φ , the tangent vectors of the two bifurcated trapping horizons overlap and is timelike. A Cauchy-foliated region is trapped if $ml^{1/4}>2^43^{-3/4}5^{-5/4}$. Fig. 3 shows a representative case of the spacetime evolving from a horizonless wormhole to a black hole and back via evaporation, depicting a horizon h_+^f that is null at $\beta, \gamma, \delta, \zeta$, spacelike in segments (β, γ) and (δ, ζ) , and timelike elsewhere; other cases are omitted for brevity.

A spacetime with globally trapped future. Given the conditions that $h \to -\infty$ as $t \to \infty$ with finite $\partial_r f$, and that the spacetime cannot be asymptotically flat but may be globally hyperbolic, we can explicitly construct the metric with the requirement that when h=0 it reduces to Ellis–Bronnikov wormhole. The ansatz $f=-1/(\sqrt{r^2+a^2}-L), h=-kt^2-mk, \mathcal{R}=L-1/(f+h), F=(f-h+nk)^2$ then yields

$$ds^{2} = \left(\frac{f - h + nk}{f + h}\right)^{2} \left(-dt^{2} + dr^{2}\right) + \left(L - \frac{1}{f + h}\right)^{2} d\Omega^{2},$$
(8)

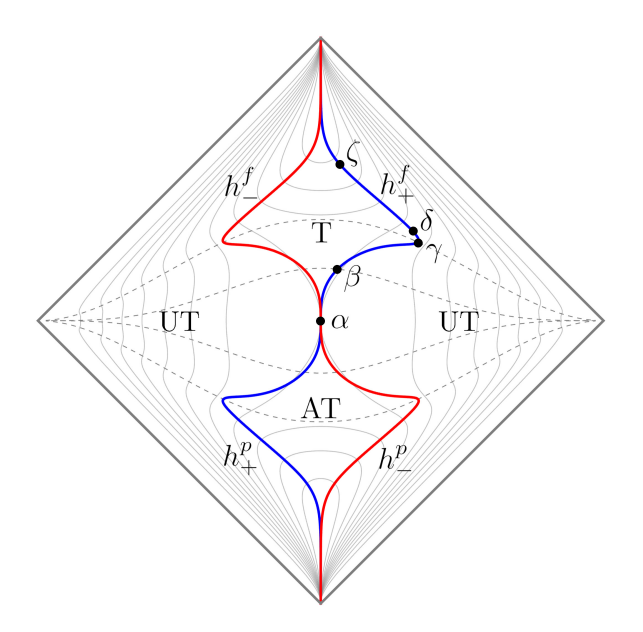


FIG. 3: Penrose diagram for a = 1, m = 0.5, l = 2. NEC and SEC are satisfied between the upper and lower dashed lines.

with $a>L>0, b, m, n, k\geq 0$. This spacetime exhibits three asymptotic regimes: a wormhole (s=+1) for k=0 or $t\to 0$; a spacetime with A=1 and $\mathcal{R}=L$ $(s=\pm 1)$ for $t\to \infty$, where $\mathscr{L}=\ln(FL^2)/L^2$ (with $F=2g^2/L^4, 2g^2=L^2$), $V=2/L^2$, and p=0, consequently making V act as a cosmological constant; and a bounce (s=-1) for $r\to 0$ or $r\to \infty$.

Let us define the throat size at t=r=0 as $\mathcal{R}_c=L+1/((a-L)^{-1}+mk)$, its infimum as $\mathcal{R}_i=L$, and its supremum as $\mathcal{R}_s=L+1/mk$. Furthermore, the regularity condition $A\neq 0$ requires mk+nk>1/(a-L) for non-zero k, implying that only one of the parameters m or n is necessary. This leads to two distinct cases: with n=0, we find $\mathcal{R}_c>(\mathcal{R}_i+\mathcal{R}_s)/2$; with m=0, we obtain $\mathcal{R}_c=a$ and $\mathcal{R}_s\to +\infty$. In both scenarios, R_s is attained at t=0 and as $r\to\infty$. In the limit $r\to\infty$ and over the range $t\to-\infty$ to $t\to +\infty$, \mathcal{R} expands from L to a finite maximum and back for n=0, whereas for m=0, it expands to infinity before returning to L. The horizon behavior as $r\to 0$ is: spacelike for $k>1/(2a(a-L)^2)$, null for $k=1/(2a(a-L)^2)$, and timelike for $k<1/(2a(a-L)^2)$.

This spacetime is globally hyperbolic despite the absence of conformal boundaries. Its Penrose-Carter diagram (Fig. 4) illustrates the process whereby a GSLBH comes to trap the entire future spacetime. The horizonless wormhole case is omitted, as it is given by the simple substitution of kt^2 in h with lt^4 .

Results and Discussion. We derive a general metric (Eq. (3)) from reasonable assumptions by solving the Einstein equations. We demonstrate three possi-

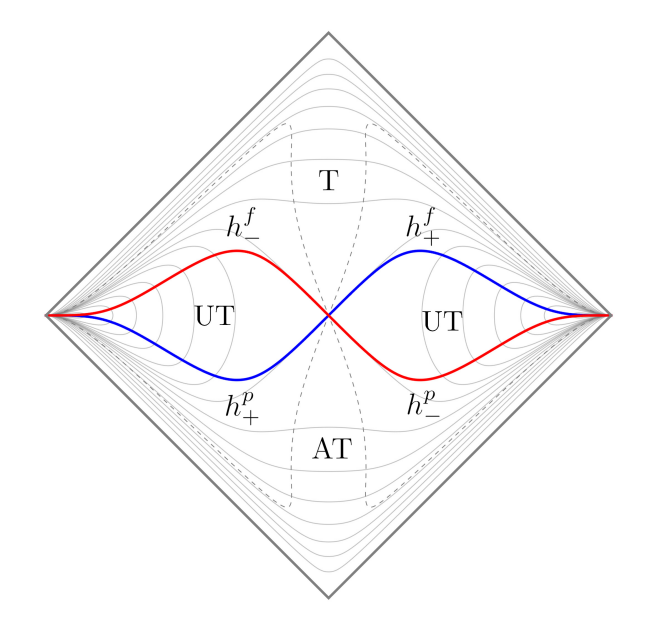


FIG. 4: Penrose diagram for $a=2, L=1, k=1/(2a(a-L)^2), mk=4, n=0$. Note that the thick gray lines do not represent conformal boundaries but merely coordinate boundaries, while the thin gray lines indicate surfaces of constant \mathcal{R} ; closer to the boundaries, these surfaces correspond to smaller \mathcal{R} . The weak energy condition (WEC) is satisfied in the region between the two dashed lines.

ble causal fates for spacetimes with future trapped regions: with only locally trapped regions; those without a globally trapped future; those without global trapping but containing bounded, Cauchy-foliated trapped regions; and those with a future that becomes completely globally trapped. Corresponding examples are given, illustrating the evolution of a GSLBH and an initially horizonless wormhole. Of particular significance is the third fate—a fully future-trapped spacetime—which constitutes a novel and consequential possibility for the evolutionary endpoint of black holes and wormholes, meriting rigorous theoretical consideration.

The general metric in Eq. (3) and the associated analysis together provide a powerful framework for the systematic construction of more complex models. By considering arbitrary functions f(r), h(r), H(f+h) and F(f-h), this formalism can be further applied to scenarios such as gravitational collapse, the evolution of multiple black holes, and dynamical wormholes. Future work should focus on identifying viable field sources of the spacetimes, as well as on their stability and thermodynamic analyses.

^{*} hrli@xjtu.edu.cn

- [1] K. Schwarzschild, Über das gravitationsfeld einer kugel aus inkompressibler flüssigkeit nach der einsteinschen theorie, Sitzungsberichte der königlich preußischen Akademie der Wissenschaften zu Berlin , 424 (1916).
- [2] R. M. Wald, General relativity (University of Chicago press, 2024).
- [3] R. Penrose, Gravitational collapse and space-time singularities, Physical Review Letters 14, 57 (1965).
- [4] S. W. Hawking, The occurrence of singularities in cosmology. iii. causality and singularities, Proceedings of the Royal Society of London. Series A. Mathematical and Physical Sciences 300, 187 (1967).
- [5] S. W. Hawking and R. Penrose, The singularities of gravitational collapse and cosmology, Proceedings of the Royal Society of London. A. Mathematical and Physical Sciences 314, 529 (1970).
- [6] J. Bardeen, Non-singular general relativistic gravitational collapse, in *Proceedings of the 5th International* Conference on Gravitation and the Theory of Relativity (1968) p. 87.
- [7] E. Ayon-Beato and A. Garcia, Regular black hole in general relativity coupled to nonlinear electrodynamics, Physical review letters 80, 5056 (1998).
- [8] E. Ayon-Beato and A. Garcia, The bardeen model as a nonlinear magnetic monopole, Physics Letters B 493, 149 (2000).
- [9] K. Bronnikov, Comment on "regular black hole in general relativity coupled to nonlinear electrodynamics", Physical review letters 85, 4641 (2000).
- [10] K. A. Bronnikov, Regular magnetic black holes and monopoles from nonlinear electrodynamics, Physical Review D 63, 044005 (2001).
- [11] A. Burinskii and S. R. Hildebrandt, New type of regular black holes and particlelike solutions from nonlinear electrodynamics, Physical Review D 65, 104017 (2002).
- [12] Z.-Y. Fan and X. Wang, Construction of regular black holes in general relativity, Physical Review D 94, 124027 (2016).
- [13] M. E. Rodrigues, M. V. de S. Silva, and H. A. Vieira, Bardeen-kiselev black hole with a cosmological constant, Physical Review D 105, 084043 (2022).
- [14] M.-A. Dariescu, C. Dariescu, V. Lungu, and C. Stelea, Kiselev solution in power-maxwell electrodynamics, Physical Review D 106, 064017 (2022).
- [15] K. A. Bronnikov, Regular black holes sourced by nonlinear electrodynamics, in Regular Black Holes: Towards a New Paradigm of Gravitational Collapse (Springer, 2023) pp. 37–67.
- [16] C. Moreno and O. Sarbach, Stability properties of black holes in self-gravitating nonlinear electrodynamics, Physical Review D 67, 024028 (2003).
- [17] M. Novello, V. De Lorenci, J. Salim, and R. Klippert, Ge-

- ometrical aspects of light propagation in nonlinear electrodynamics, Physical Review D **61**, 045001 (2000).
- [18] M. Novello, S. P. Bergliaffa, and J. Salim, Singularities in general relativity coupled to nonlinear electrodynamics, Classical and Quantum Gravity 17, 3821 (2000).
- [19] M.-S. Ma and R. Zhao, Corrected form of the first law of thermodynamics for regular black holes, Classical and Quantum Gravity 31, 245014 (2014).
- [20] A. Bokulić, I. Smolić, and T. Jurić, Black hole thermodynamics in the presence of nonlinear electromagnetic fields, Physical Review D 103, 124059 (2021).
- [21] A. Simpson and M. Visser, Black-bounce to traversable wormhole, Journal of Cosmology and Astroparticle Physics 2019 (02), 042.
- [22] F. S. Lobo, M. E. Rodrigues, M. V. d. S. Silva, A. Simpson, and M. Visser, Novel black-bounce spacetimes: wormholes, regularity, energy conditions, and causal structure, Physical Review D 103, 084052 (2021).
- [23] K. Bronnikov, Black bounces, wormholes, and partly phantom scalar fields, Physical Review D 106, 064029 (2022).
- [24] K. A. Bronnikov and R. K. Walia, Field sources for simpson-visser spacetimes, Physical Review D 105, 044039 (2022).
- [25] P. Cañate, Black bounces as magnetically charged phantom regular black holes in einstein-nonlinear electrodynamics gravity coupled to a self-interacting scalar field, Physical Review D 106, 024031 (2022).
- [26] S. A. Hayward, Dynamic wormholes, International Journal of Modern Physics D 8, 373 (1999).
- [27] H.-a. Shinkai and S. A. Hayward, Fate of the first traversible wormhole: Black-hole collapse or inflationary expansion, Physical Review D 66, 044005 (2002).
- [28] S. A. Hayward, Wormhole dynamics in spherical symmetry, Physical Review D—Particles, Fields, Gravitation, and Cosmology 79, 124001 (2009).
- [29] K. Bronnikov, H. Dehnen, and V. Melnikov, Regular black holes and black universes, General Relativity and Gravitation 39, 973 (2007).
- [30] S. A. Hayward, Formation and evaporation of regular black holes, Phys. Rev. Lett. 96, 031103 (2006), arXiv:gr-qc/0506126.
- [31] A. Simpson, P. Martin-Moruno, and M. Visser, Vaidya spacetimes, black-bounces, and traversable wormholes, Classical and Quantum Gravity 36, 145007 (2019).
- [32] F. S. Lobo, A. Simpson, and M. Visser, Dynamic thinshell black-bounce traversable wormholes, Physical Review D 101, 124035 (2020).
- [33] J. Yang and H. Huang, Trapping horizons of the evolving charged wormhole and black bounce, Physical Review D 104, 084005 (2021).
- [34] A. Ashtekar, Geometry and physics of null infinity, arXiv preprint arXiv:1409.1800 (2014).